Supplementary Materials

Flexible, Self-healing and Portable Supramolecular Visualization Smart Sensors for Monitoring and Quantifying Structural Damage

*Dezhi Jiao[a], Sihan Gu[a], Li Cheng[b], Shuoqi Li[a], Chengbao Liu[a]**

[a]*College of Materials Science and Engineering, Shandong University of Science and Technology, Qingdao 266590, China*

[b]*Laboratory of Advanced Rubber Material, Ministry of Education (Type B), Qingdao University of Science and Technology, Qingdao 266042, China*

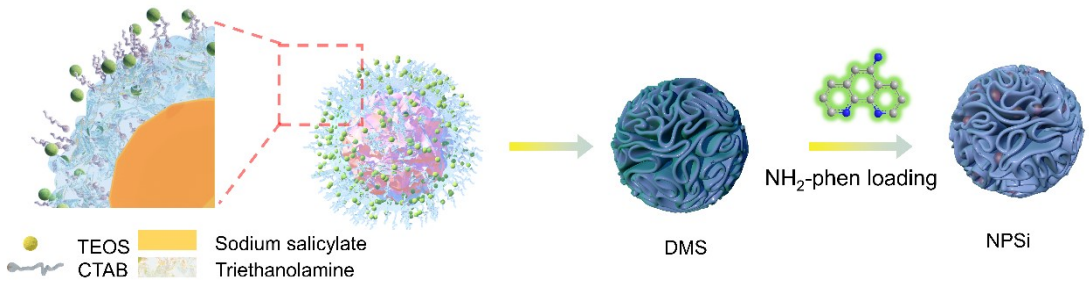

Fig. S1. The procedure schematic of preparation DMS and NPSi.

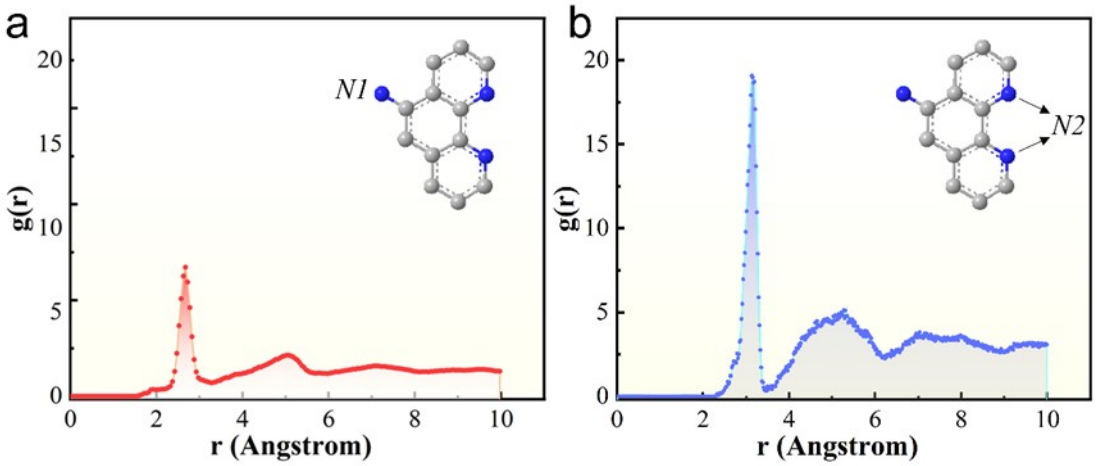

Fig. S2. The relevant RDF analysis of NH_2-Phen molecule (a) NH_2-Phen-N1 and (b) NH_2-Phen-N2.

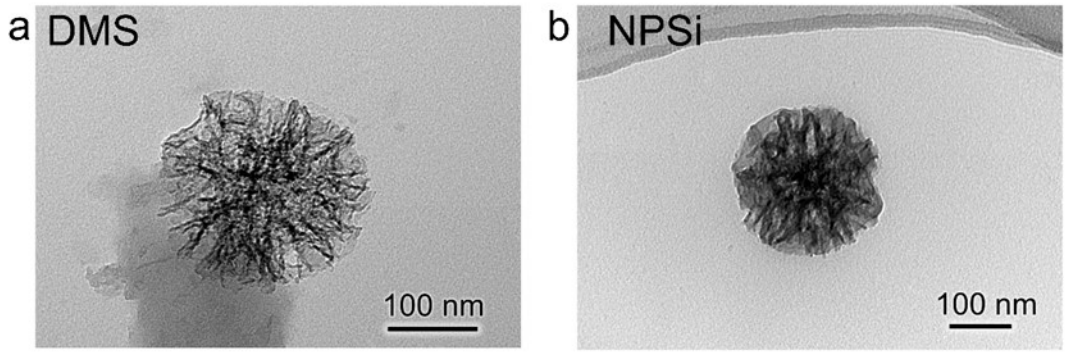

Fig. S3. TEM images of (a) DMS and (b) NPSi.

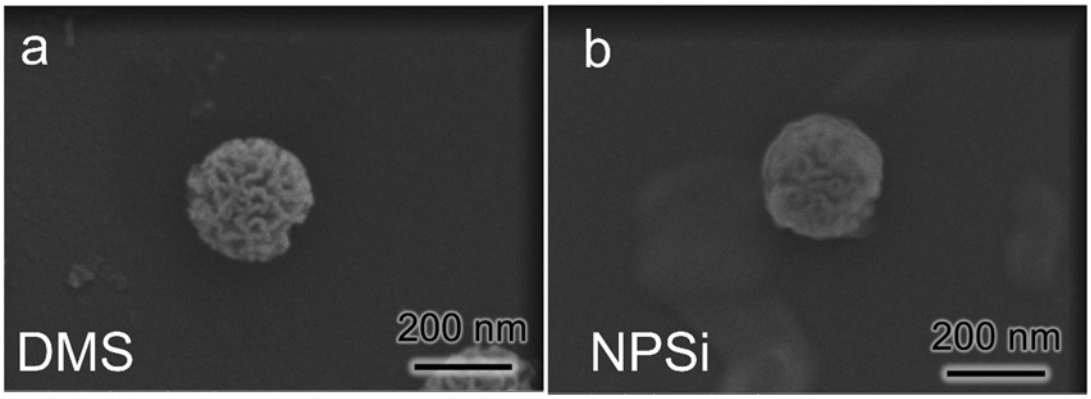

Fig. S4. SEM results of (a) DMS and (b) NPSi.

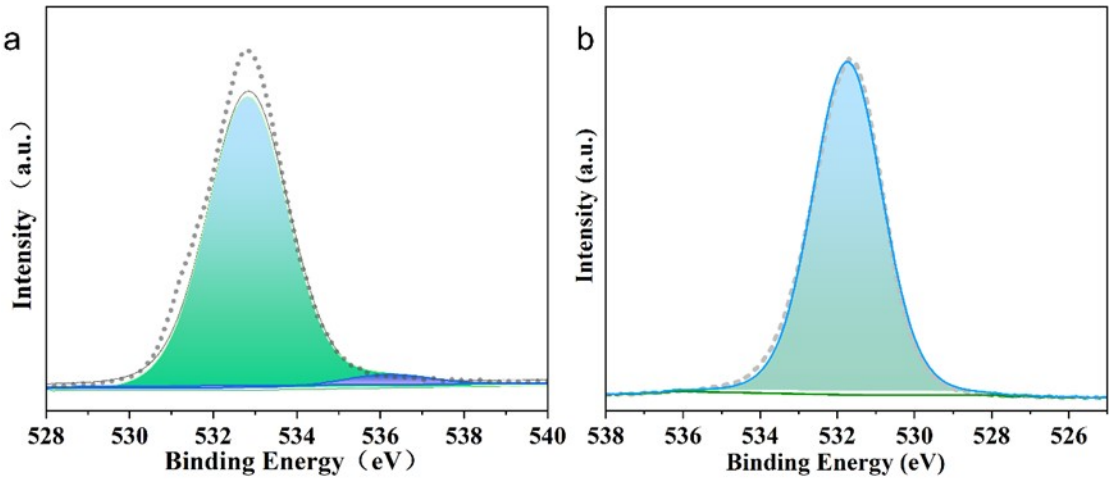

Fig. S5. XPS fine spectra (O 2p) of (a) NPSi and (b) DMS.

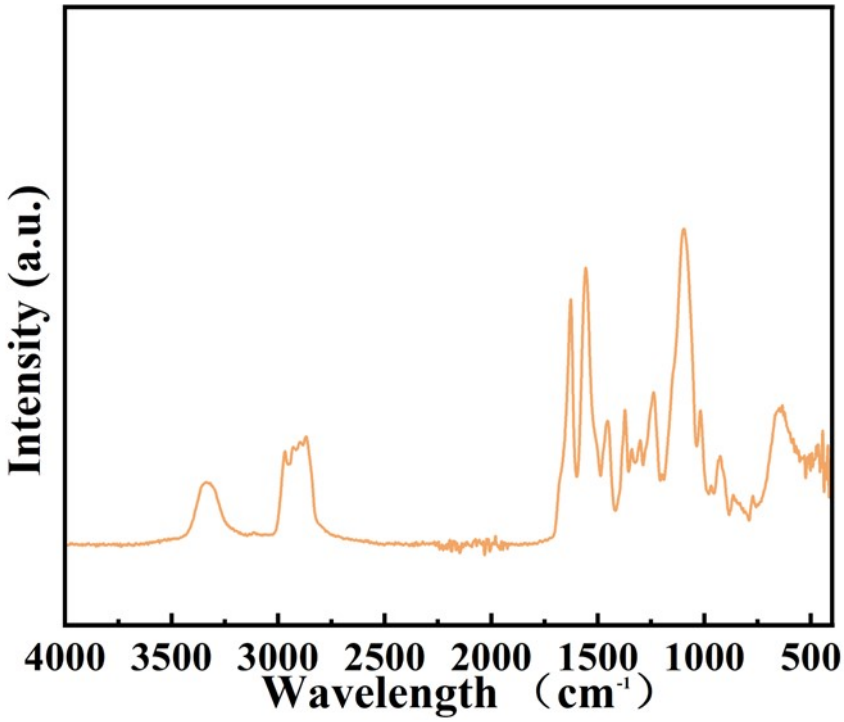

Fig. S6. Infrared spectra of the PU.

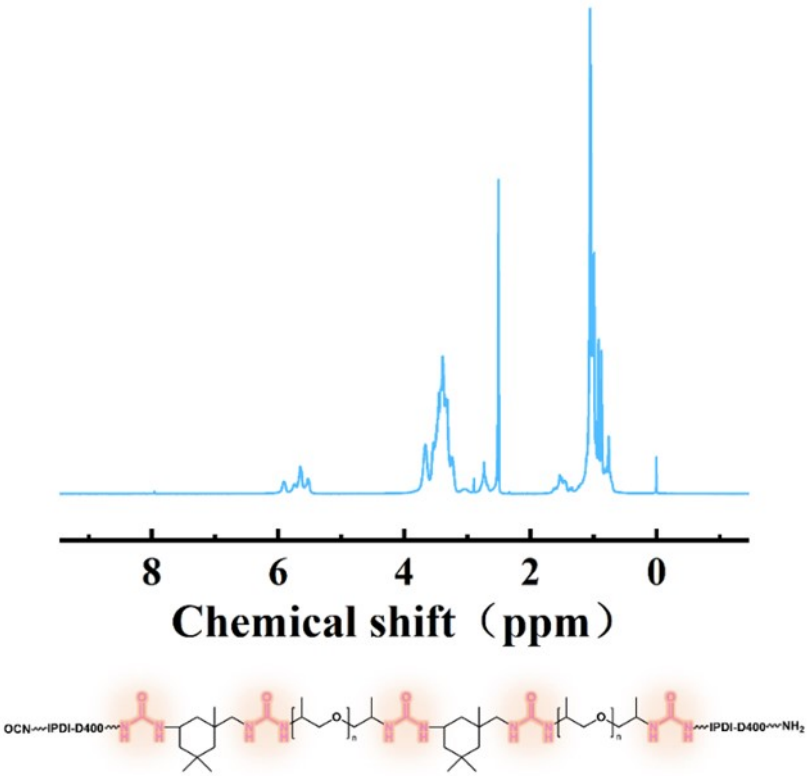

Fig. S7. ^{1}H NMR spectra of PU.

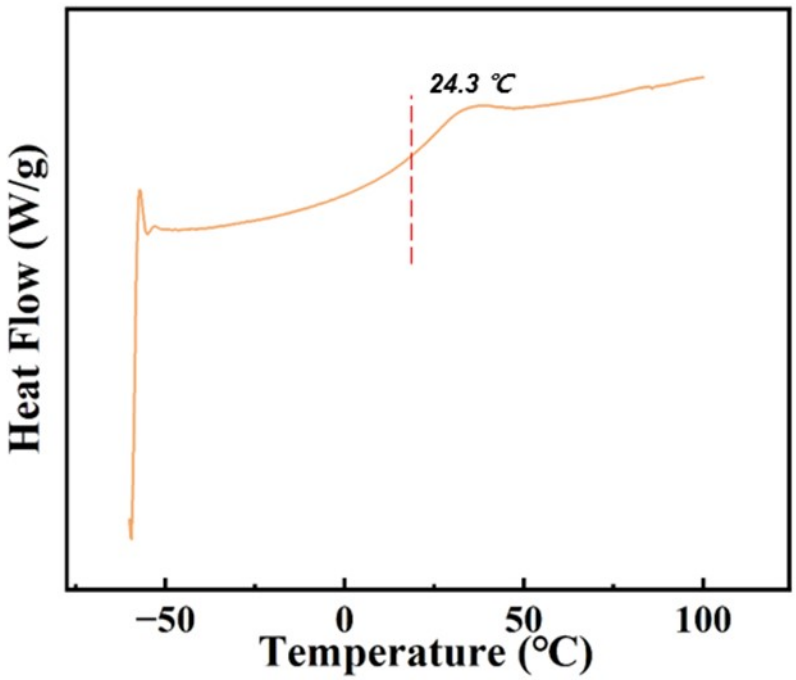

Fig. S8. DSC thermograms of PU.

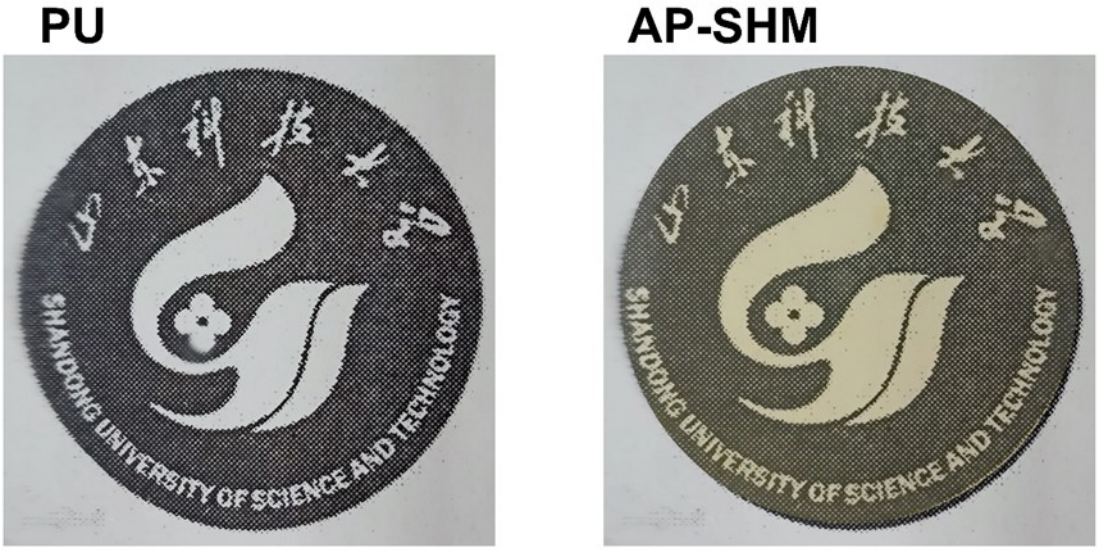

Fig. S9. Optical photograph of PU and AP-SHM.

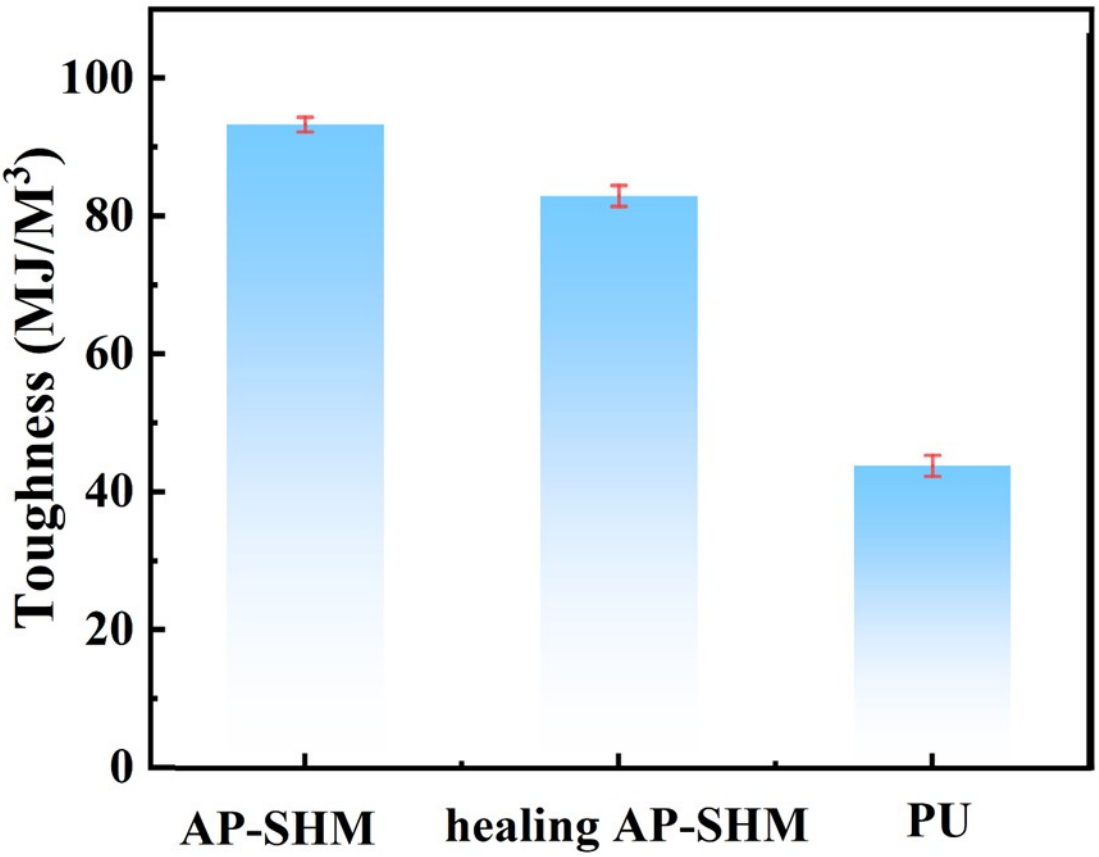

Fig. S10. The toughness of AP-SHM, healing AP-SHM, and PU.

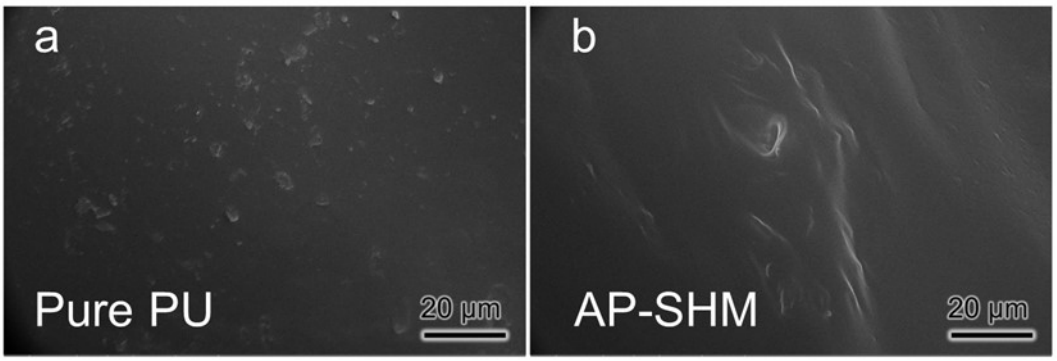

Fig. S11. SEM images of cross-section of (a) Pure PU and (b) AP-SHM.

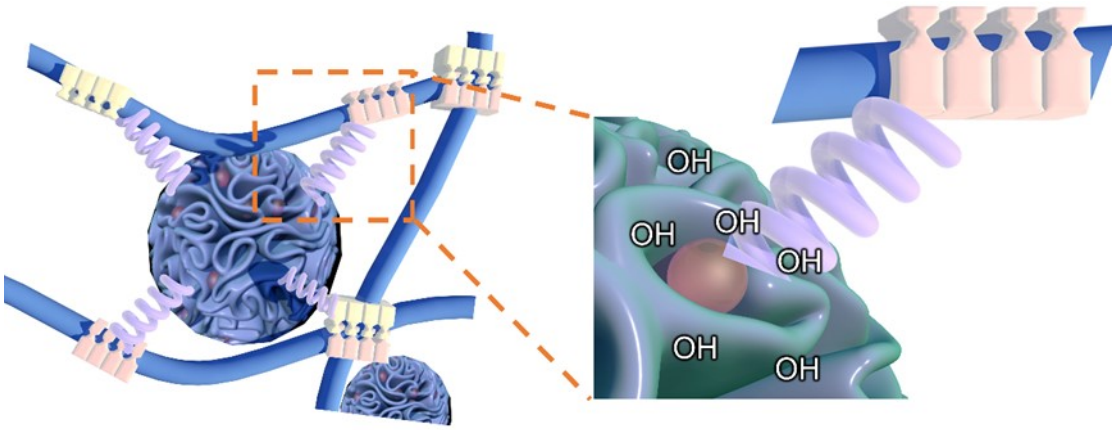

Fig. S12. The interaction mechanism between NPSi and PU molecule chain.

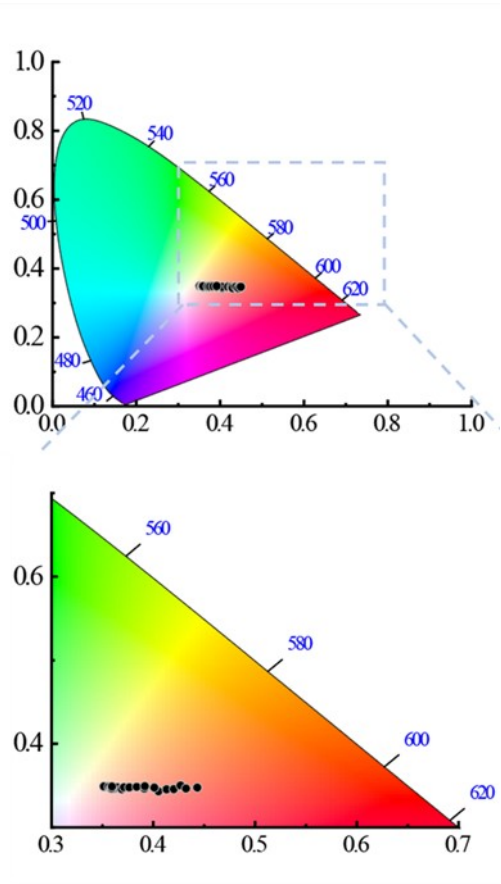

Fig. S13. chromaticity coordinate of FeTP with the addition of different concentrations of Fe^{2+}.

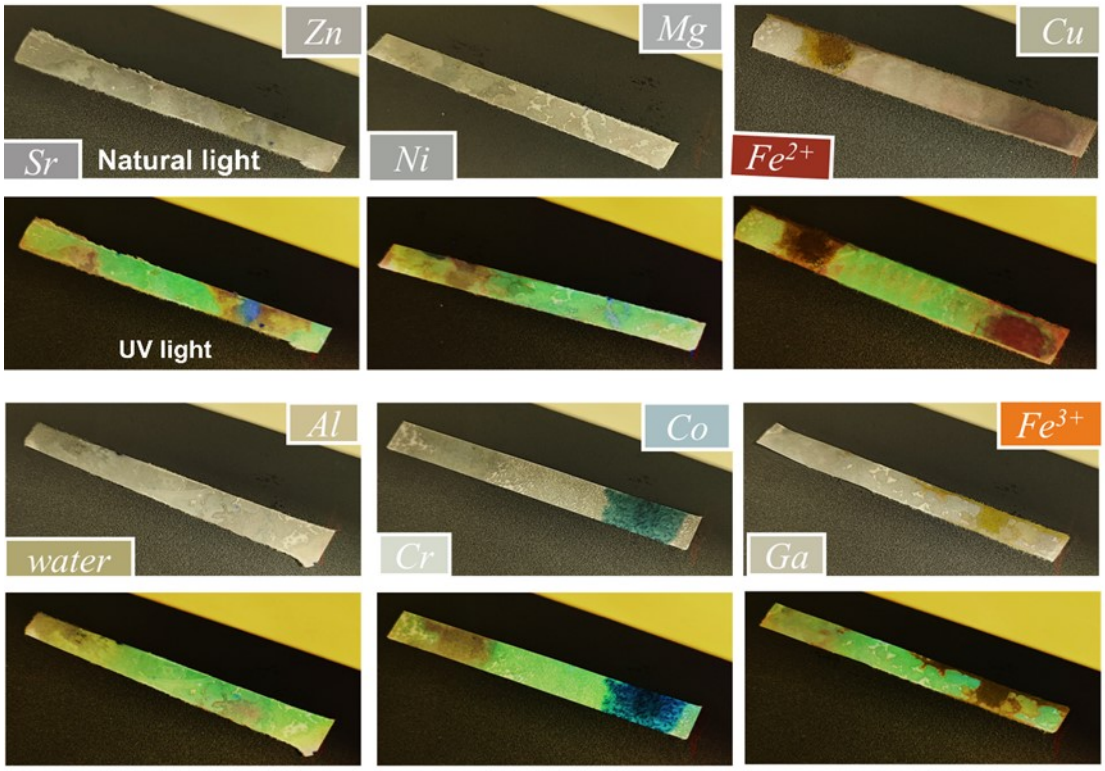

Fig. S14. Optical photograph of the FeTP addition with the equal concentration cation (Al^{3+}, Mg^{2+}, Cu^{2+}, Cr^{3+}, Ni^{2+}, Co^{2+}, Fe^{3+}, Fe^{2+}, Sr^{2+}, Zn^{2+}) in UV mode and vis mode.

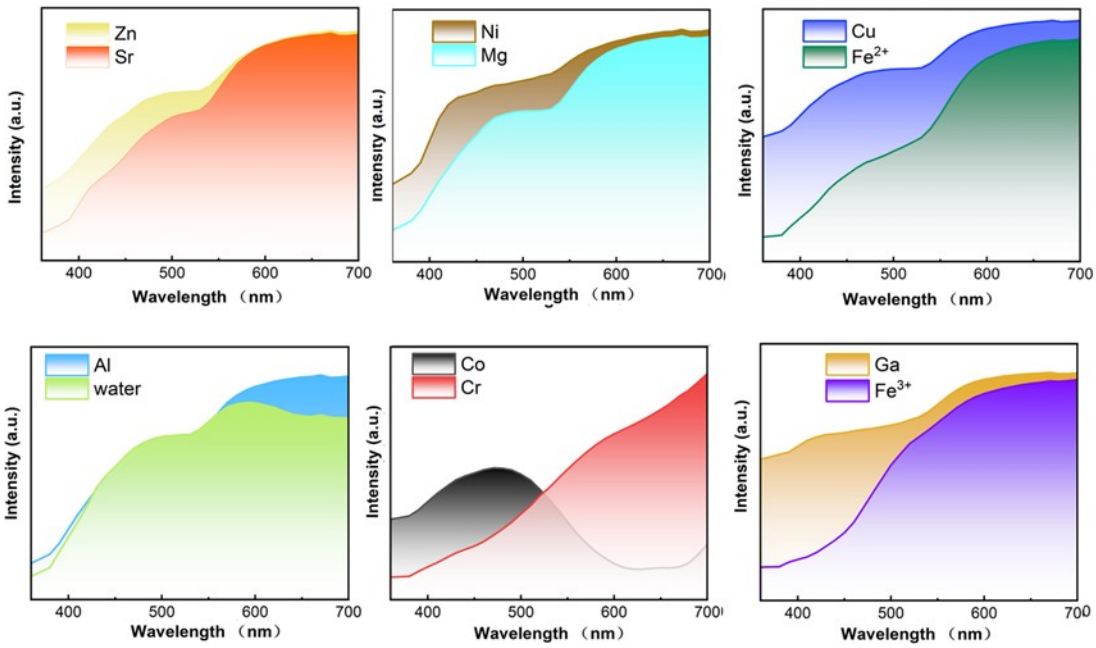

Fig. S15. UV-visible spectrum of the FeTP addition with the equal concentration cation (Al^{3+}, Mg^{2+}, Cu^{2+}, Cr^{3+}, Ni^{2+}, Co^{2+}, Fe^{3+}, Fe^{2+}, Sr^{2+}, Zn^{2+}).

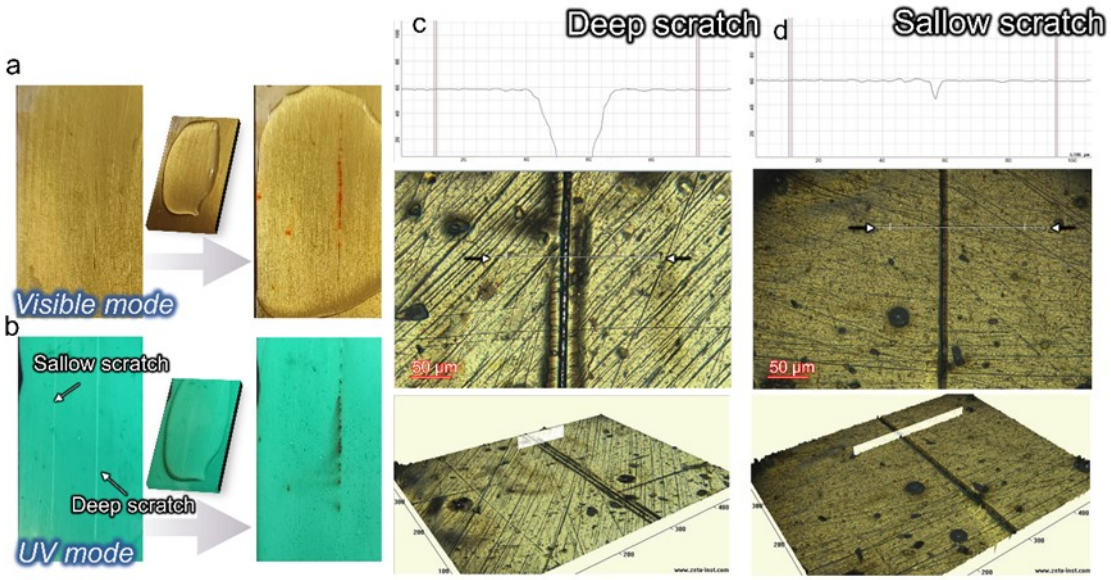

Fig. S16. Optical photographs of different types of scratches on AP-SHM in (a) visble mode and (b) UV mode; The 3D morphology results of scratches on AP-SHM: (c) deep scratch and (d) sallow scratch.

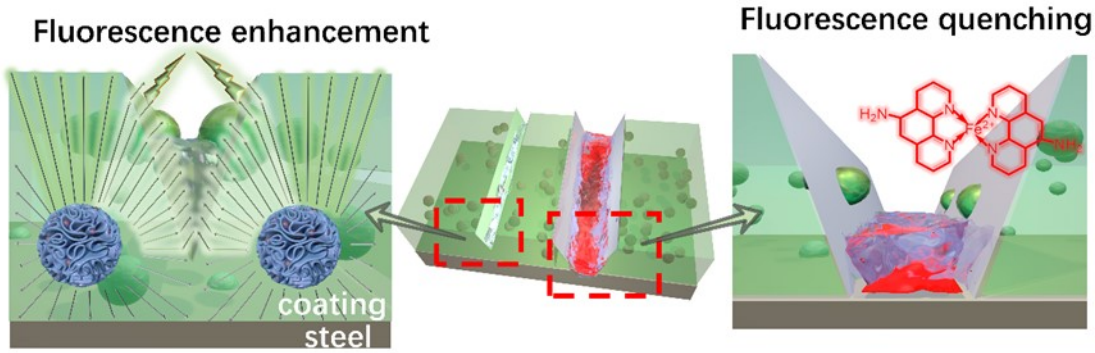

Fig. S17. Schematic diagram of damage-induced enhancement mechanism.

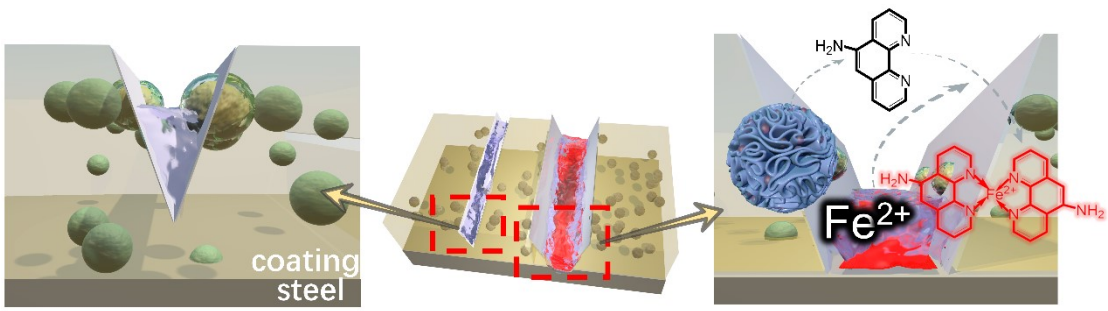

Fig. S18. Schematic diagram of ion recognition quenching mechanism.

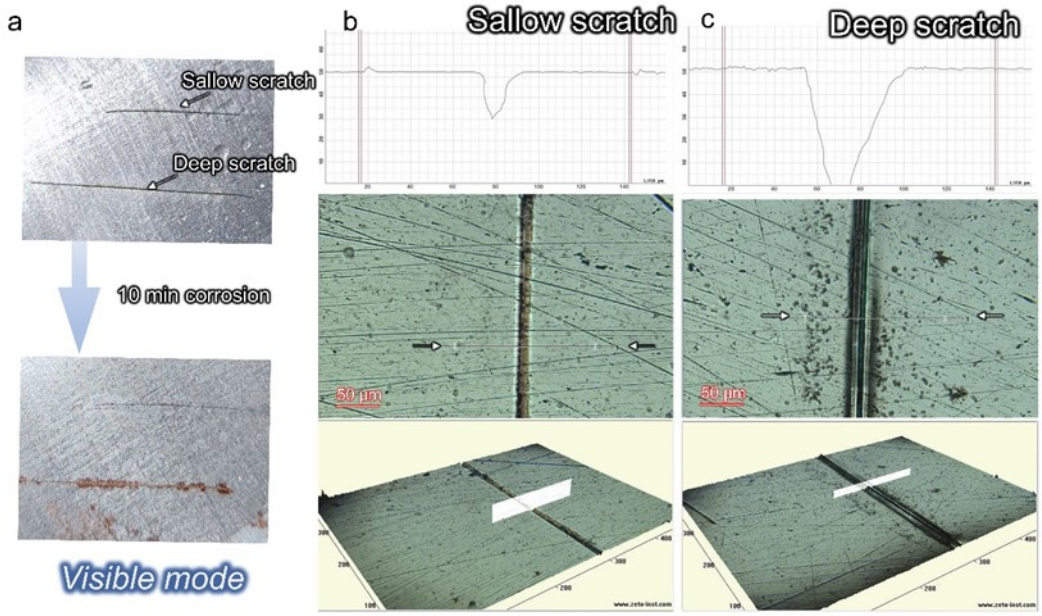

Fig. S19. Optical photographs of different types of scratches on PU; The 3D morphology results of different types of scratches on PU.

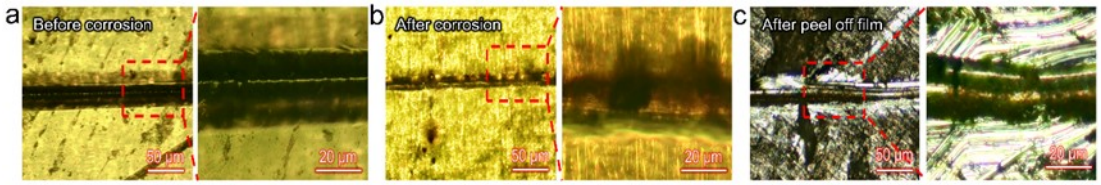

Fig. S20. Optical microscope photographs of (a) before corrosion, (b) after corrosion, and c) after peel off film for deep scratch.

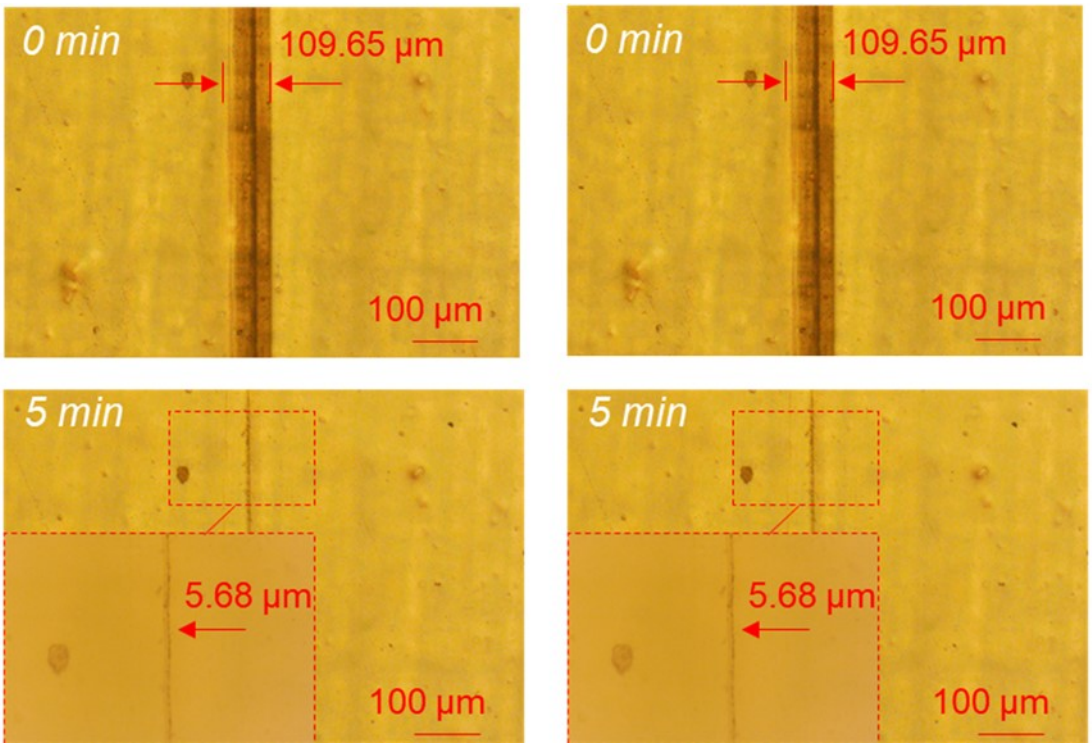

Fig. S21. The self-healing process of coated AP-SHM sample.

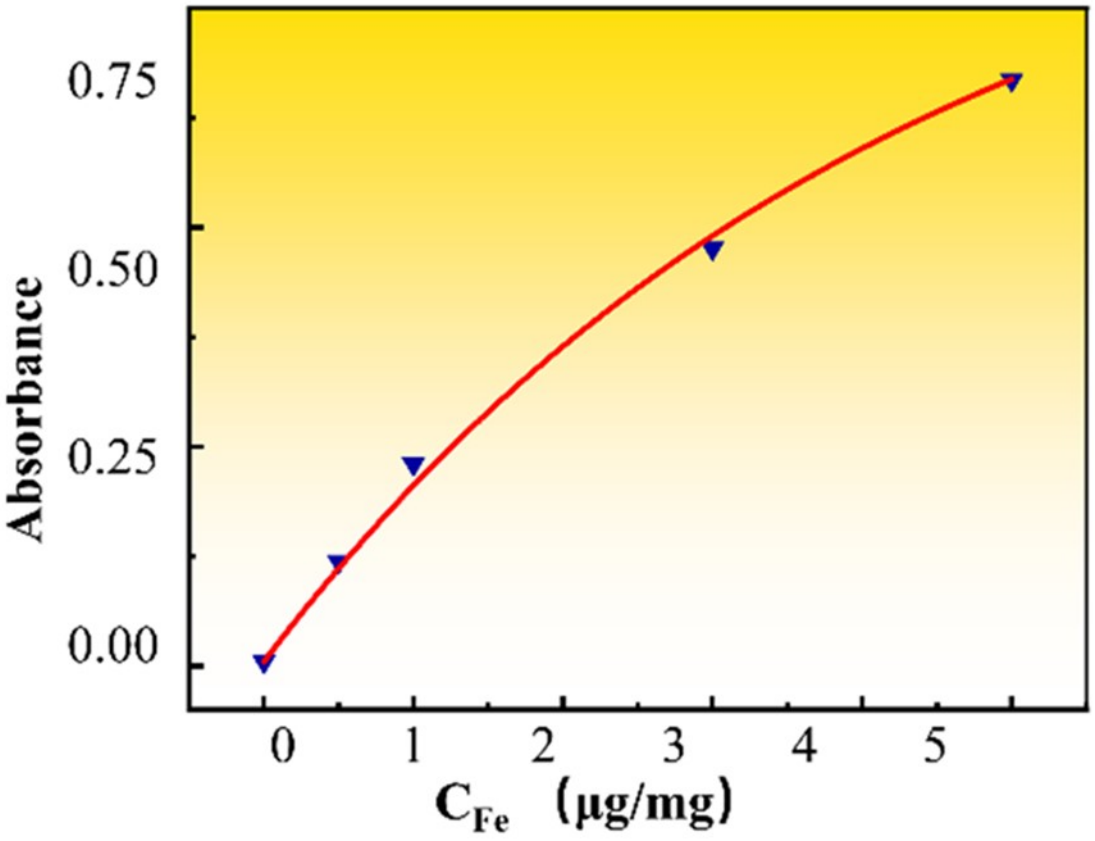

Fig. S22. Concentration-absorbance curve of elemental iron standard solution.

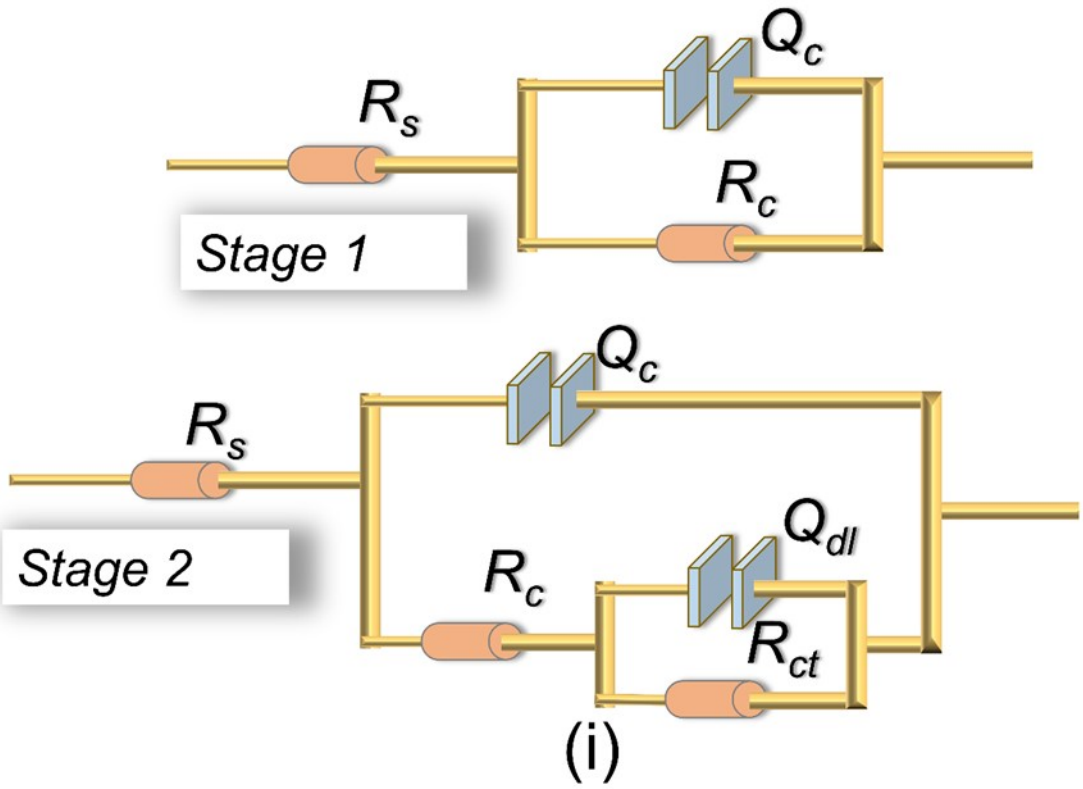

Fig. S23. Electrical equivalent circuit models.

Table S1 EIS fitting parameters for stage 1.

Time (d)	0.04	0.1	0.2	0.3	0.4
R_s($\Omega \cdot cm^2$)	5.67	6.41	6.33	5.91	6.35
CPE ($\mu\Omega^{-1} \cdot cm^{-2} \cdot S^n$)	1.73	2.175	2.2	2.61	2.81
n	0.82	0.78	0.79	0.77	0.75
R_f($\Omega \cdot cm^2$)	1126	1362	2452	1201	1979
χ^2 (10^{-3})	2.51	1.93	1.56	2.26	3.95

Table S2 EIS fitting parameters for stage 2 and 3.

Equation		$Y_{FAAS}=A_1e^{\frac{-x}{t_1}}+A_2e^{\frac{-x}{t_2}}+Y_0$			$Y_{c\text{-}G}=A_1e^{\frac{-x}{t_1}}+A_2e^{\frac{-x}{t_2}}+Y_0$			$Y_{Z\text{-}c}=A_1e^{\frac{-x}{t_1}}+Y_0$		
Time (d)		0.5	1	1.5	2	3	4	5	6	7
	Y_0		0.973			4.427×10^{6}			3.072	
R_s(Ω·cm^2)		6.1	6.57	5.96	6.47	6.61	6.01	5.43	5.59	5.58
	A_1		-0.484			-9.396×10^{-4}			3.252×10^{30}	
CPE_1 (μΩ^{-1}·cm^{-2}·S^n)		2.09	2.47	2.33	1.70	1.53	1.95	1.83	1.78	2.04
	t_1		3.901			-0.487			3.006	
n_1		0.74	0.74	0.74	0.76	0.74	0.71	0.71	0.72	0.71
	A_2		-0.484			-4.426×10^{6}			-	
R_c(Ω·cm^2)		11.42	13.42	8.68	6.26	8.63	10.17	6.48	10.91	10.91
	t_2		4.769			-3.411×10^{5}			-	
CPE_2 (μΩ^{-1} cm^{-2} S^n)		0.75	0.75	0.89	1.28	0.72	0.56	1.18	0.48	0.56
	R^2		0.998			0.987			0.974	
n_2		0.86	0.88	0.88	0.83	0.89	0.94	0.84	0.97	0.92
R_{ct} (Ω·cm^2)		1639	1611	1465	2348	2680	3018	3754	2271	2107
χ^2 (10^{-4})		4.37	6.13	7.87	6.28	6.09	6.44	6.217	9.11	5.22

Table S3 Algorithmic fitting equations and parameters.

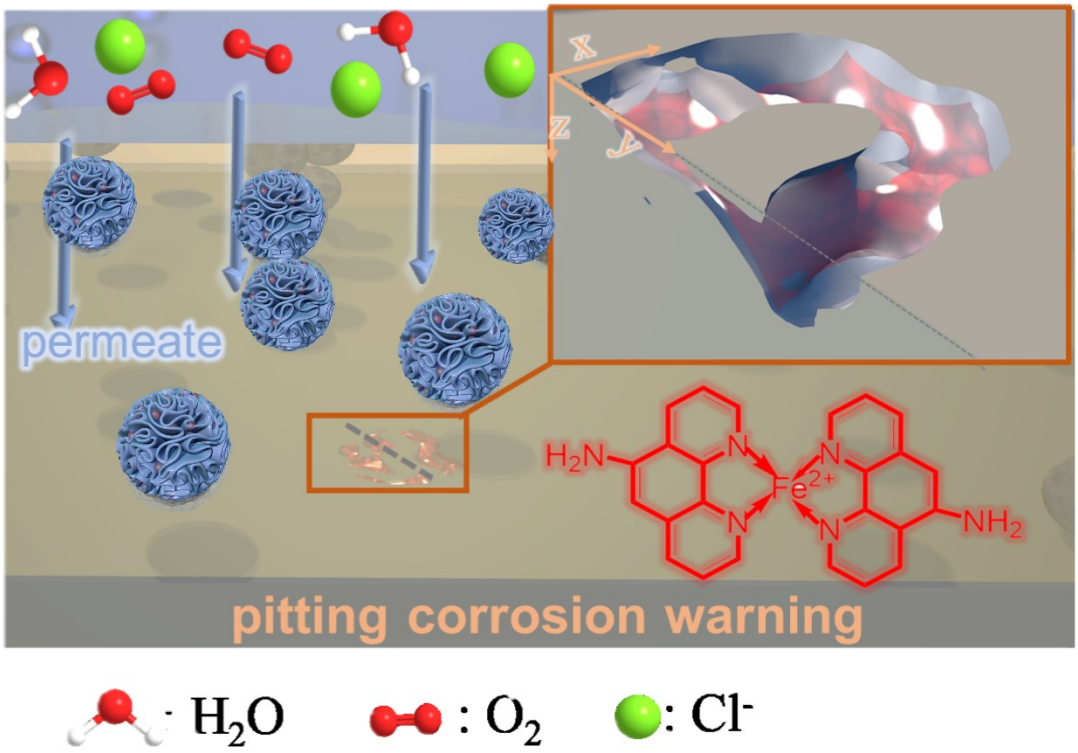

Fig. S24. Schematic diagram of AP-SHM pitting corrosion warning.

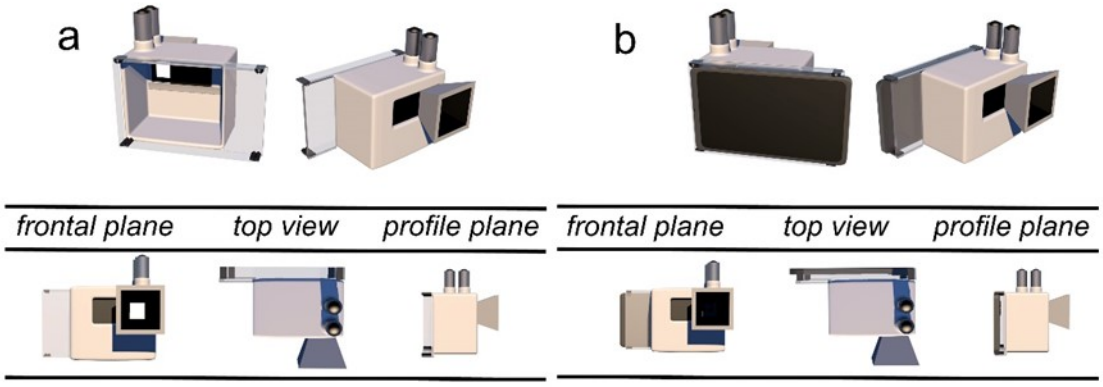

Fig. S25. (a) The portable detachable device that assist with image acquisition; (b) the integrated portable device with image capture platform.

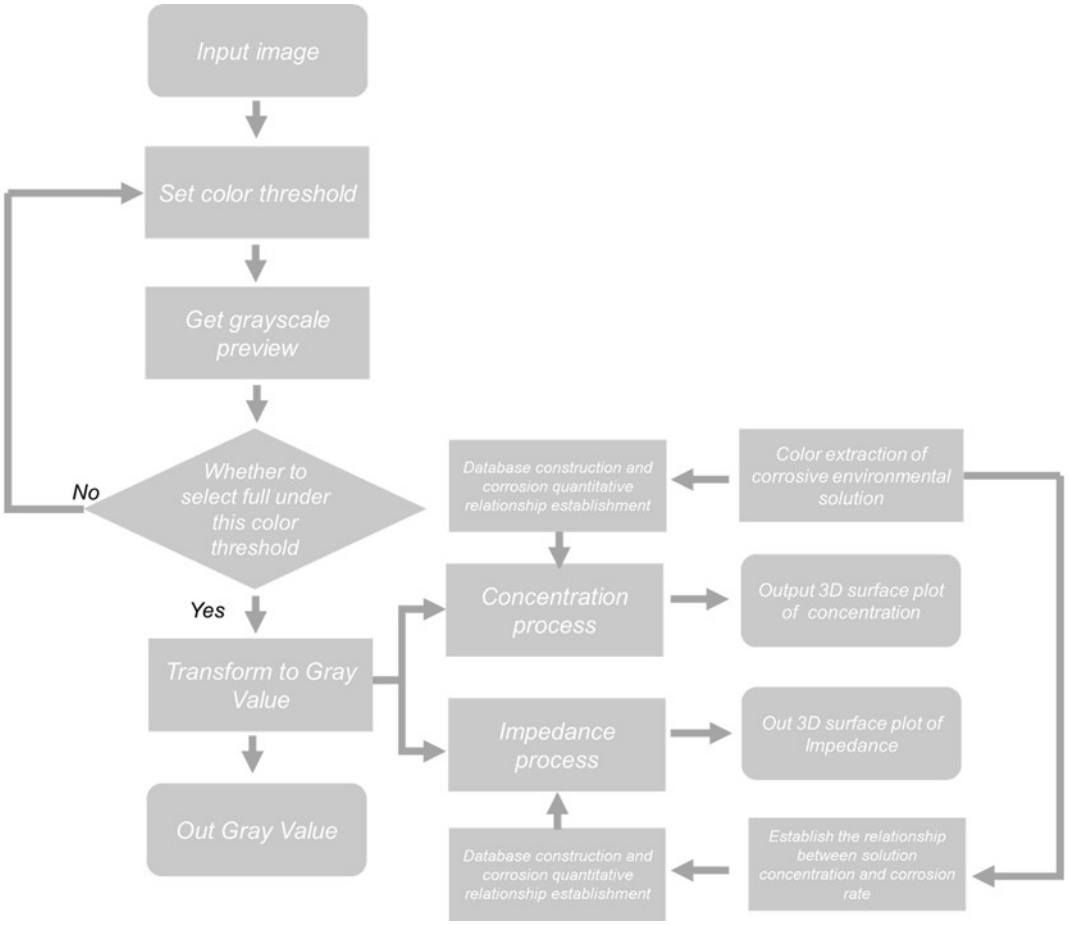

Fig. S26. Diagram of software AI algorithm.

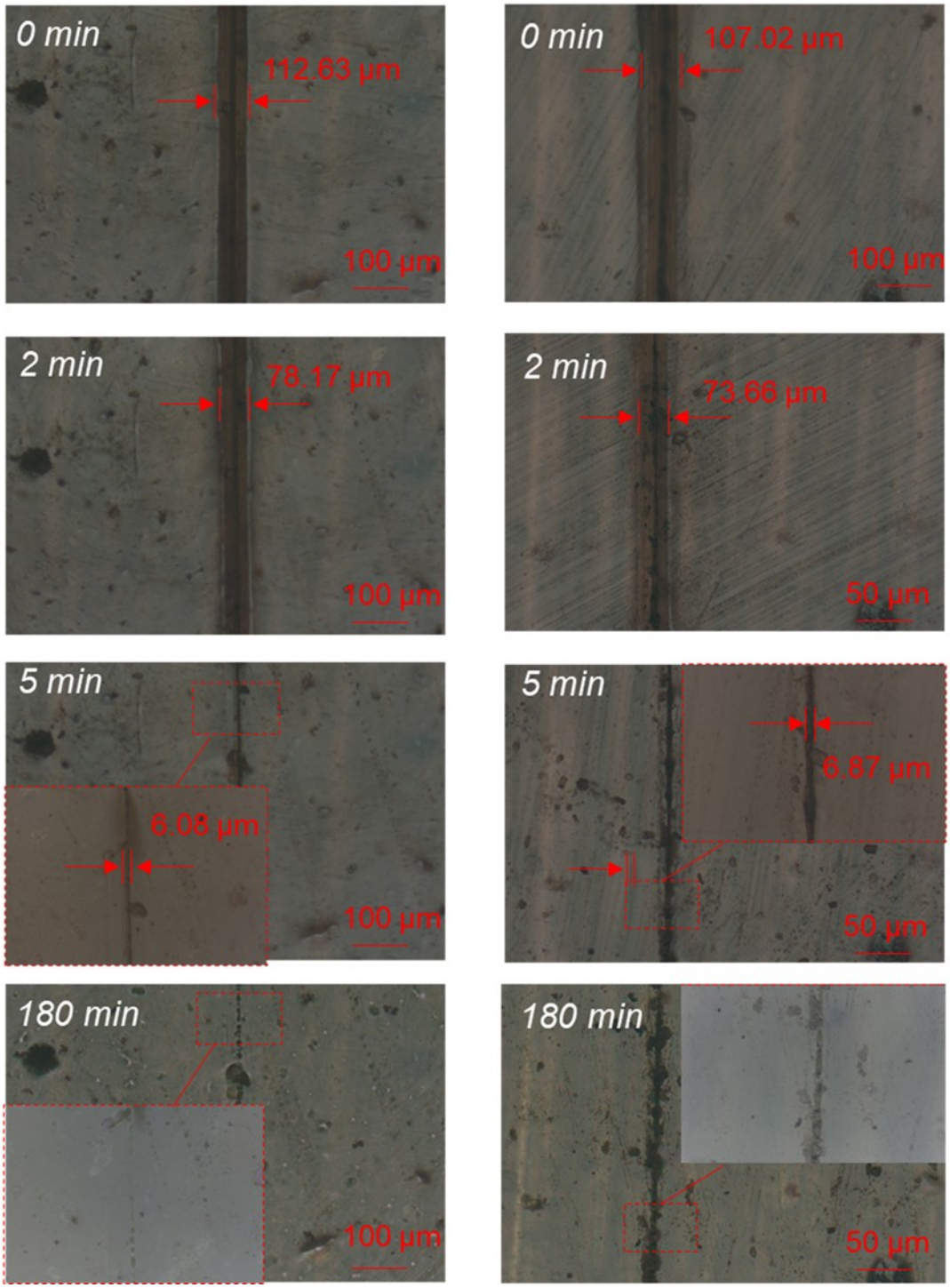

Fig. S27. The specific healing process of AP-SHM that exposed in a) spray test and b) -10 ℃

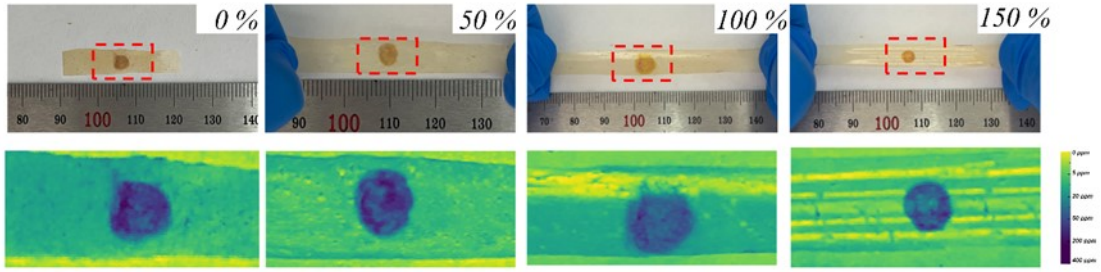

Fig. S28. Responsiveness of AP-SHM under stretchable strain.

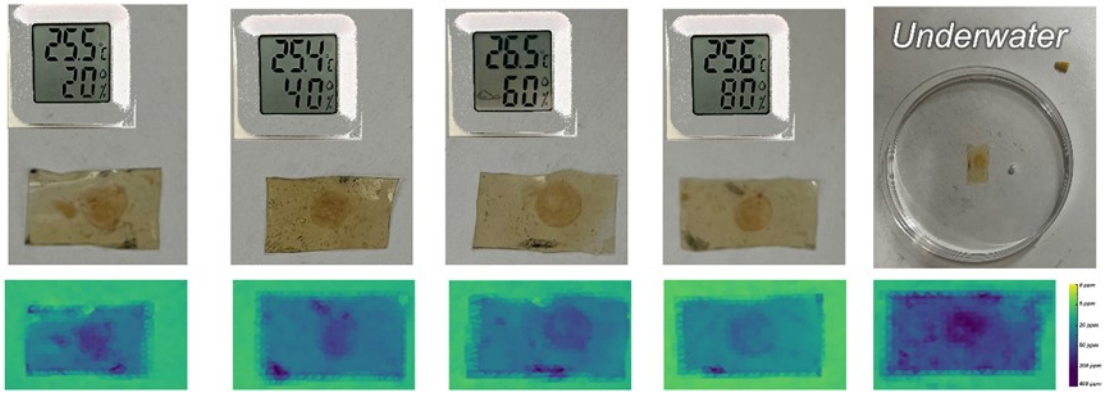

Fig. S29. Responsiveness of AP-SHM under different humidity.

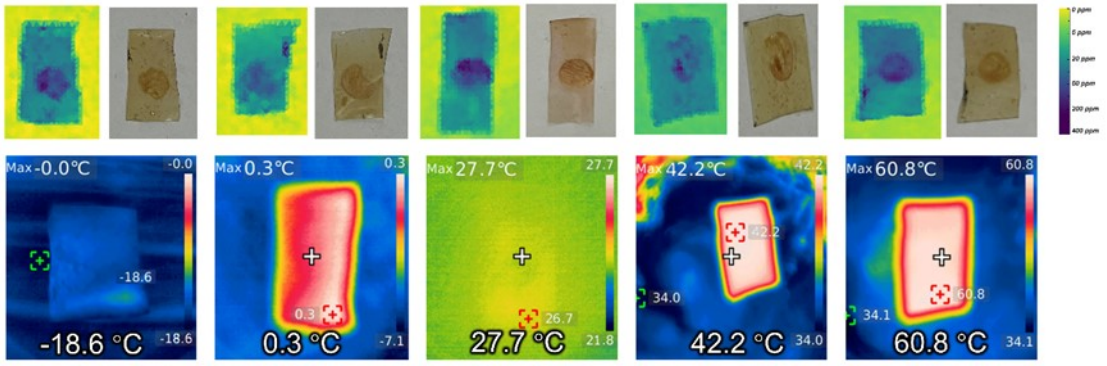

Fig. S30. Responsiveness of AP-SHM under different temperature.

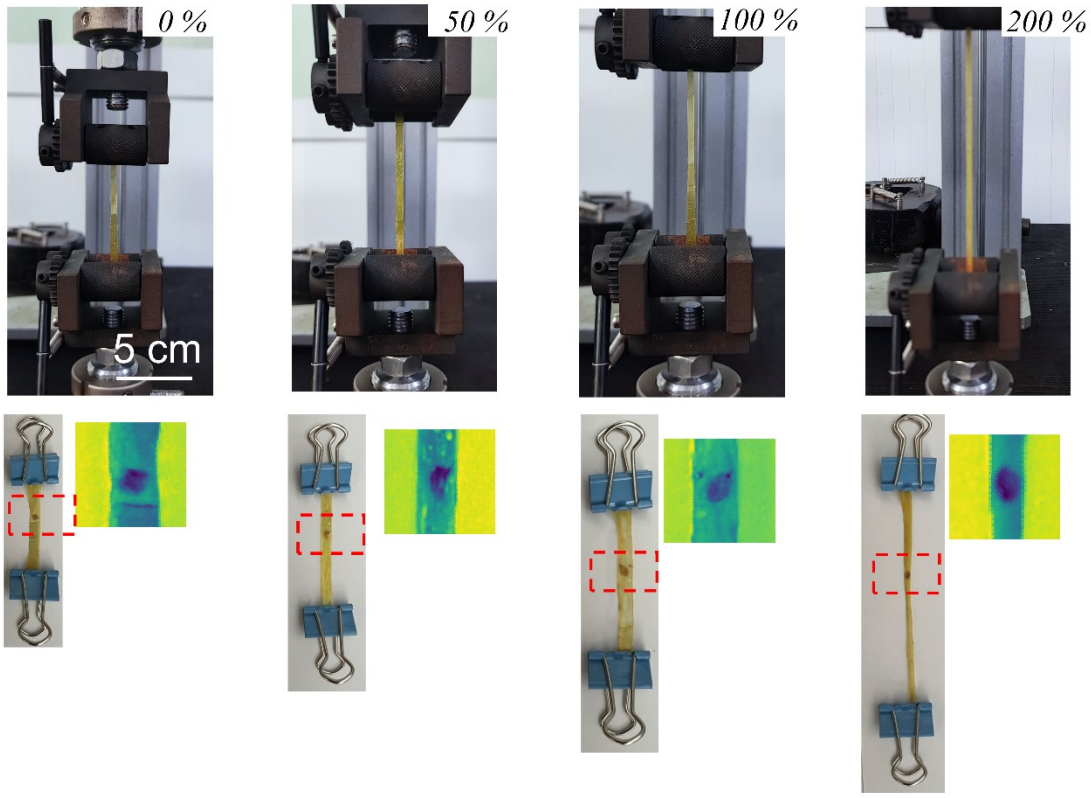

Fig. S31. Continuous stretching with different degrees of deformation for one week.